

Fatigue Behavior of Welded Joints in a Ferritic Stainless Steel SUS444

Masaki NAKAJIMA¹, Masayuki AKITA², Keiro TOKAJI³ and Yousuke TAKAI⁴

¹Department of Mechanical Engineering, Toyota College of Technology, Toyota 471-8525, Japan

²Faculty of Engineering, Gifu University, Gifu 500-1193, Japan

³Department of Mechanical and Systems Engineering, Gifu University, Gifu 500-1193, Japan

⁴Toshiba Industrial Products Manufacturing, Co., Asahi-cho, Mie-prefecture 510-8521, Japan

ABSTRACT

Fatigue behavior was studied on welded joints of a ferritic stainless steel, SUS444. Push-pull fatigue tests were conducted using plate specimens with the weld zone at the center of gauge section. Fatigue crack propagation (FCP) tests were also conducted using two types of CT-specimens with a starter notch in the heat-affected zone (HAZ) and in the weld metal. The fatigue strength of the welded specimens decreased remarkably compared to that of the base specimens, SUS444. In order to clarify the cause of the reduction in fatigue strength, additional fatigue tests were carried out using annealed welded specimens and smooth welded specimens in which the excess weld was removed. The fatigue strength of the annealed welded specimens was slightly improved, indicating that residual stress exerted a little influence on the fatigue strength of the welded specimens. On the other hand, the fatigue strength of the smooth welded specimens was nearly the same as that of the base specimens. Based on these results and FEM analysis of the welded zone, it was concluded that the decrease in fatigue strength of the welded specimens was attributed to the stress concentration at the toe of weld. In the welded specimens, multiple cracks were generated at the toe of weld and then coalesced, but the crack growth could not be measured owing to the shape of the excess weld. Early crack growth was measured using the smooth welded specimens. In early crack growth region, the discernible difference was found between the base specimens and the smooth welded specimens, i.e. the crack growth rates of the base specimens were faster than those of the smooth welded specimens. With increasing crack size, the $da/dN-\Delta K$ relationships for small cracks gradually approached the $da/dN-\Delta K_{\text{eff}}$ relationships for long cracks and then coincided with them.

1 INTRODUCTION

High-purity ferritic stainless steels with extremely reduced (C + N) contents have been developed, whose toughness and weldability are significantly improved^{1), 2)}. With the improvement, new ferritic stainless steels are used in various engineering fields. For further extensive applications, it is necessary to clarify their mechanical properties, but there existed a very few studies on the fatigue properties³⁾. In addition, the evaluation on fatigue properties of welded joints is particularly important to ensure the safety and reliability of machine components and structures. However, studies on the fatigue properties of welded joints in new ferritic stainless steels have been limited.

In the present study, fatigue behavior was studied on welded joints of a ferritic stainless steel, SUS444. The obtained results were discussed on the basis of residual stress, stress concentration and crack

growth behavior.

2 EXPERIMENTAL PROCEDURES

2.1 Material and specimens

The material used in the present study is a ferritic stainless steel, SUS444 (18Cr-2Mo), whose chemical composition (mass %) is C: 0.004, Si: 0.06, Mn: 0.1, P: 0.024, S: 0.006, Ni: 0.11, Nb: 0.17, Cr: 18.72, Mo: 1.81, V: 0.06, N: 0.068, Fe: Bal.. The mechanical properties for the L and T directions are listed in Table 1. The proof stress and tensile strength in the T direction are slightly higher than those in the L direction.

Table 1: Mechanical properties of the base metal.

Direction	0.2%proof stress	Tensile strength	Breaking strength on final area	Elongation	Reduction of area
	^{0.2} (MPa)	^B (MPa)	^T (MPa)	ϕ (%)	ψ (%)
L	293	445	1480	34	83
T	310	460	1352	31	81

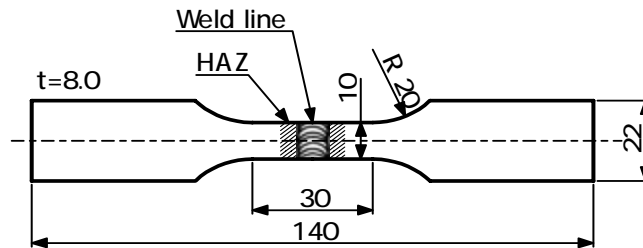


Figure 1: Specimen configuration (mm).

The configuration of plate specimen for *S-N* tests is shown in Fig.1. The specimen has weld line normal to the longitudinal direction (welded specimen). Two types of welded CT specimens, i.e. the specimens in which the starter notch was introduced within HAZ (H-specimen) and within the weld metal (W-specimen) respectively, were also prepared for long crack propagation tests. Since the welding direction was parallel to the T direction, the crack growth direction was parallel to the T direction in plate specimens and CT specimens.

2.2 Welding condition

Welding was conducted by the tungsten-inert gas (TIG) welding method with a root opening of 1.6mm, an X-shape groove, the voltage of 20V and three welding passes on both sides. The filler metal was an austenitic stainless steel, SUS309L.

Before experiments, microstructure and hardness around the weld zone were examined. As a result, the average grain size was 56 μ m and 123 μ m for the base metal and HAZ, respectively and Vickers

hardness was $HV162$, $HV172$ and $HV194$ for the base metal, HAZ and weld metal, respectively.

2.3 Experimental procedures

Fatigue tests were performed using electro-hydraulic fatigue testing machines at a stress ratio of -1 and a frequency of 10Hz for $S-N$ tests, and at 0.05 and 1Hz for long crack propagation tests. Crack length was measured by replicating method for small cracks and by traveling microscope for long cracks. Crack closure was measured by an unloading elastic compliance method. After experiments, fracture surfaces were observed using a scanning electron microscope (SEM).

3 RESULTS

3.1 Residual stress distribution

Residual stress for the welded specimens was measured by the X-ray diffraction method. The distribution of residual stress in the L direction normal to the weld line is shown in Fig.2. Residual stresses are approximately $-250 \sim -450\text{MPa}$ at the top surface (the side of the first pass), while are $70 \sim 170\text{MPa}$ at the bottom surface (the opposite side of the second pass). The residual stresses are almost constant over the distance measured.

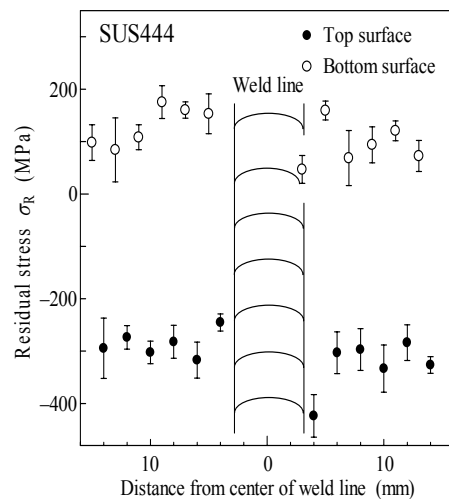


Figure 2: Distribution of residual stress in L direction.

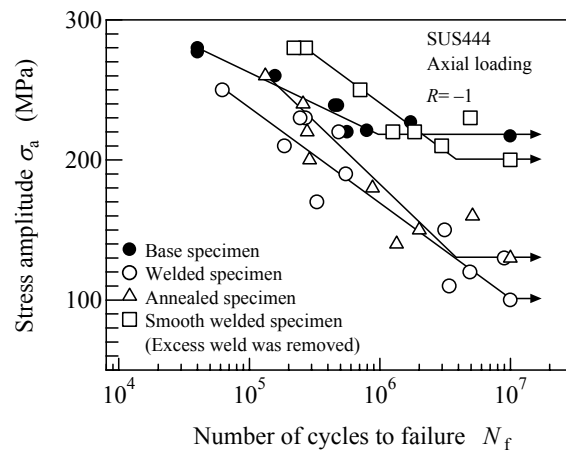


Figure 3: $S-N$ diagram.

3.2 Fatigue strength

The $S-N$ curve of the welded specimens is shown in Fig.3. For comparison, the $S-N$ curve for the base metal, SUS444, is also represented in the figure (hereafter, base specimen). The fatigue strength of the welded specimens decreases remarkably compared to that of the base specimens, i.e. the fatigue limit is lowered from 220MPa to 100MPa . Since the decrease in fatigue strength was thought to be due to residual stress induced by welding and stress concentration at the toe of weld, additional fatigue tests were performed using annealed welded specimens and specimens in which the excess weld was removed (hereafter, smooth welded specimen). The results obtained are included in Fig.3. As can be seen, the

fatigue strength of the annealed specimen is slightly improved in comparison with that of the welded specimens, i.e. fatigue limit increases to 130MPa. This indicates that residual stress exerts a little influence on the decrease in fatigue strength of the welded specimens. On the other hand, the fatigue strength of the smooth welded specimens increases at high stress levels compared to the base specimens and the fatigue limit is nearly the same as that of base specimens. Based on these results, it is considered that the decrease in fatigue strength of the welded specimens is attributed to the stress concentration at the toe of weld.

4 DISCUSSION

4.1. Stress concentration at the toe of weld

In the welded specimens, multiple cracks were generated at the boundary between the excess weld and the base metal, i.e. at the toe of weld, and then coalesced. Stress concentration at the toe of weld was analyzed by means of two-dimensional FEM. FEM analysis was performed several times on the geometries simulated the actual shape of the weld zone, because the actual shapes of the toe of weld were different in each specimen. Typical examples of FEM analysis are shown in Fig.4. The stress concentration factors, K_t , obtained are ranged from 1.6 to 2.9, and the average value of K_t is approximately 2.25. As mentioned above, because of such a high stress concentration at the toe of weld, cracks always initiated at the toe of weld. When the value of K_t is assumed as 2.25, the fatigue limit of about 98MPa can be estimated for the welded specimen, which value is coincident with the experimental results of 100MPa.

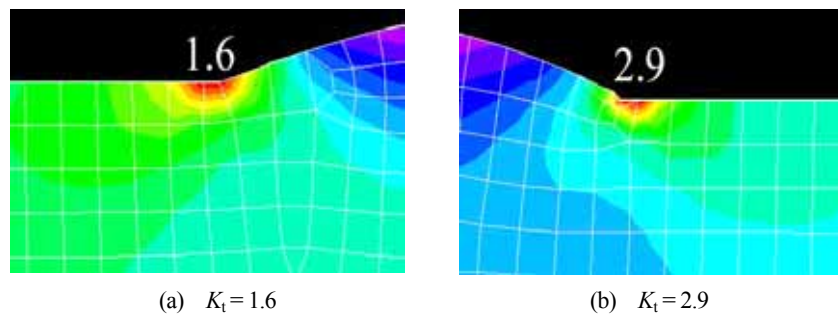


Figure 4: Examples of FEM analysis on stress concentration at the toe of weld.

4.2. Fatigue crack growth behavior

Figure 5 represents a SEM micrograph of crack initiation site in a welded specimen. The flat ductile facet is observed at the crack initiation site, while the unevenness of fracture surface is also seen around it. In macroscopic view of fracture surfaces, several ratchet marks were observed. This suggests that multiple cracks were generated at the toe of weld and then coalesced in the welded specimens. Because of a complicated geometry of the weld zone, crack growth could not be measured. Thus smooth welded specimens were used to examine the early crack growth in the weld zone.

The relationship between crack growth rate, dc/dN , and half crack length on the specimen surface, c , is shown in Fig.6. In early crack growth region, there is a remarkable difference in dc/dN between the base

specimens and the smooth welded specimens, where the crack growth rates in the smooth welded specimens were slower than those of the base specimens. This result corresponds with the fatigue strength seen in $S-N$ diagram (Fig.3), where the fatigue strength of the smooth welded specimens increased in comparison with the base specimens at high stress levels. As also shown in Fig.6, the fluctuation of dc/dN in the region of crack size below $400\mu\text{m}$ is remarkable, indicating that the early crack growth just after the crack initiation is strongly influenced by microstructure.

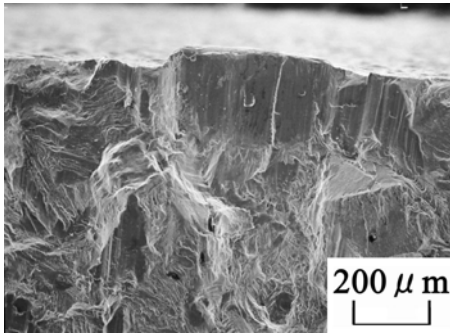


Figure 5: Microscopic view of crack initiation site in welded specimen.

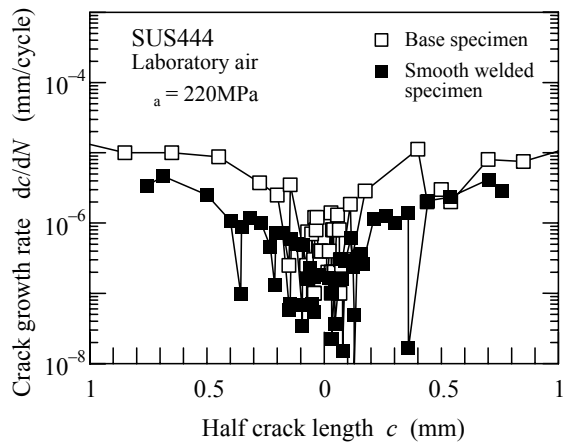


Figure 6: Relationships between dc/dN and c for small cracks.

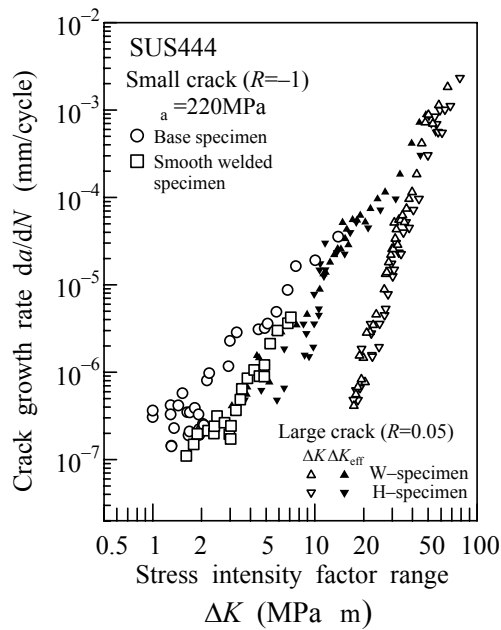


Figure 7: Relationships between da/dN and K for small cracks.

Figure 7 shows the relationship between crack growth rate, da/dN , and stress intensity factor range, ΔK , for small cracks⁴⁾. Since fatigue tests were conducted at a stress ratio of -1 , K_{\max} was used as ΔK . For comparison, the results for long cracks in the H- and W-specimens are also included in the figure. As seen in Fig.2, compressive residual stress of $-250 \sim -450$ MPa and tensile residual stress of $70 \sim 170$ MPa were present at the top and bottom surfaces in HAZ, respectively. Residual stress in the weld metal could not be measured. However, since the da/dN - ΔK relationships for the H- and W-specimen are almost identical, it is assumed that the similar residual stresses would be present in the weld metal. It seems that the crack growth behavior in both specimens is affected by compressive residual stress rather than tensile residual stress, because the absolute value of the former is significantly larger than that of the latter. Indeed the crack growth rates of the H- and W-specimens are lower than those for the base metal in the entire ΔK region³⁾, indicating higher crack growth resistance of HAZ and the weld metal than the base metal.

As also seen in Fig.7, small cracks propagate at the ΔK levels below the threshold stress intensity for long cracks. In addition, the crack growth rates of the base specimens are faster than those of the smooth welded specimens. With increasing crack size, the crack growth rates for small cracks in both specimens gradually approach those for long cracks, i.e. the da/dN - ΔK relationships for small cracks gradually approach the da/dN - ΔK_{eff} relationships for long cracks and then coincided with them.

5 CONCLUSIONS

Fatigue behavior was studied on welded joints of a ferritic stainless steel, SUS444. The results obtained are as follows;

(1) Fatigue strength of the welded specimens decreased remarkably compared to that of the base material, SUS444. The decrease in fatigue strength of the welded specimens was attributed to the stress concentration at the toe of weld.

(2) Crack initiation and growth in the welded specimens could not be measured owing to the geometry of the weld zone, thus crack growth was measured using the smooth welded specimens in which the excess weld was removed. In early crack growth region, the crack growth rates of the base specimens were faster than those of the smooth welded specimens. With increasing crack size, the da/dN - ΔK relationships for small cracks gradually approached the da/dN - ΔK_{eff} relationships for long cracks and then coincided with them.

REFERENCES

- 1) T.Nakazawa, S.Suzuki, T.Sunami and Y.Sogo, Application of High-Purity Ferritic Stainless Steel Plates to Welded Structures, *ASTM STP*, **706** (1980), 99.
- 2) J.D.Redmond, Toughness of 18Cr-2Mo Stainless Steel, *ASTM STP*, **706** (1980), 123.
- 3) M.Nakajima, M.Akita, K.Tokaji and T.Shimizu, Fatigue Crack Initiation and Early Growth Behavior of a Ferritic Stainless Steel in Laboratory Air and in 3%NaCl Aqueous Solution, *JSME International Journal, Ser. A*, **46** (2003), 575.
- 4) J.C.Newman,Jr., A Review and Assessment of the Stress-Intensity Factors for Surface Cracks, *ASTM STP*, **687** (1979), 16.